

COLORED SOLAR MODULES USING INTEGRATED PIXELATED RESONANT DIELECTRIC NANOSCATTERER ARRAYS

Verena Neder,^{1,2} Stefan L. Luxembourg,³ and Albert Polman²

¹Institute of Physics, University of Amsterdam

Science Park 904, 1098 XH Amsterdam, the Netherlands

²Center for Nanophotonics, AMOLF,

Science Park 104, 1098 XJ, Amsterdam, the Netherlands

³ECN Solar Energy, PO Box 1, 1755 ZG Petten, the Netherlands

ABSTRACT: Green colored photovoltaic modules based on silicon heterojunction solar cells integrated with periodic arrays of light scattering Si nanoscatterers were made. Here, we expand this concept to multiple colors and color combinations. We show that random arrays of silicon nanoarrays can be combined to pixels to create the desired color. By adjusting the coverage of pixels composed of different nanoparticle arrays different colors can be designed and the calculated chromaticity values can be obtained from the fabricated sample. The pixelated nanoscattering concept was used to realize a solar mini-module with a scattering spectrum close to white. The calculated relative loss in short-circuit current is only 19%. The nanoparticle pixel arrays can be made using soft imprint lithography opening up an alternative route for designing low loss colored PV modules.

Keywords: nanoparticles, silicon solar cell, building integration

1 INTRODUCTION

For photovoltaics (PV) to be applied on a very large scale it is essential that PV panels are well integrated into our built environment and landscape. Typically, PV panels have a black or dark blue appearance that results from the textured surface of the solar cells in combination with a dielectric antireflection (AR) coating, designed to optimize the absorption of sunlight in the solar cell. However, for building- and landscape-integrated applications it would be beneficial to have PV panels in a variety of well-defined colors, while maintaining a high PV conversion efficiency.

Recently, we have reported a new method to create a green colored solar module using resonant light scattering from silicon nanoparticles with optical Mie resonances [1]. We exploited the use of dielectric Mie scatterers, integrated with the top cover layer of a solar panel, to selectively scatter a narrow band of the solar spectrum resulting in a bright green color. In the present paper, this concept is expanded in order to achieve a broad range of colors; and to create white solar mini-modules. The reduction in short circuit current densities is only 11% for the green colored mini-modules and 19% for the white colored mini-module.

2 DIELECTRIC SCATTERERS FOR COLORATION

Dielectric nanostructures are known to have bright scattering colors due to the excitation of Mie resonances. The resonant spectrum can be tailored by particle shape and refractive index [2]. If made from low-loss dielectrics the Mie resonance can have a relatively narrow linewidth, resulting in a bright scattering spectrum with -depending on the used dielectric- negligible absorption losses. Several authors have demonstrated colorful examples of light scattering from arrays of Mie scatterers made on planar substrates [3]-[7].

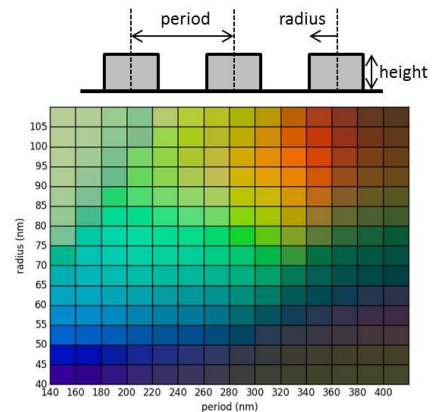


Figure 1: Color of reflection of periodic array of silicon Mie cylinders of a height of 100 nm on a sapphire substrate for different radius and period. Numerical simulations of reflection spectra were done using Lumerical FDTD and are transformed to visible color. A schematic of the geometry of the structure is shown above.

Figure 1 shows the result of numerical finite-difference-time-domain (FDTD) simulations (Lumerical) of the reflected color of square arrays of silicon nanocylinders (height 100 nm) on a semi-infinite sapphire substrate. The visual colors were obtained using the concept described in [8], using the average midday light spectrum in Western Europe (D65) as illumination source. By varying the radius and period of the Si cylinders, the Mie resonance spectrum is controlled and the color can be tuned over the entire color spectrum visible by the human eye. In Fig. 2 a photograph of a sample with six fields of silicon nanocylinder arrays of different radius and period (height ~105-110 nm) on top of sapphire is shown. The fabrication was done by electron beam lithography and reactive ion etching of a planar silicon-on-sapphire substrate. The measured scattering spectra of the fields in Fig. 2a are plotted in Fig. 2b and show that with increasing radius and period the Mie resonances are shifting to larger wavelengths. The simulated reflectance spectra (height 105 nm) plotted in the same figure match well with the

experiment. The scattering bandwidth is determined by the scattering rate and absorption losses in the nanoparticles and varies over the shown spectral range.

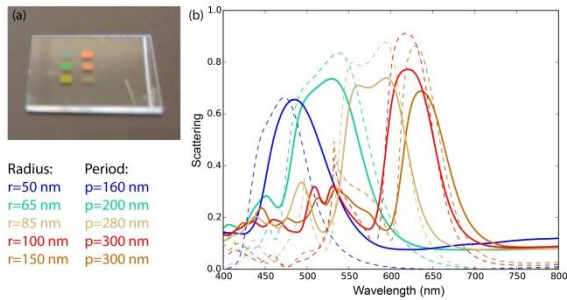


Figure 2: (a) Photograph of 6 fields of periodic arrays of silicon cylinders on top of a sapphire substrate with different radius and period (height 105-110 nm). Radius and periods of the simulated arrays are indicated. They match with ± 10 nm the fabricated dimensions. (b) Measured (solid lines) and simulated (dashed lines) scattering spectra of 5 colored fields.

3 PRINTED SINGLE COLORED SOLAR CELL

To integrate the Mie scattering effect into a solar module, the nanopatterned sapphire cover slides with periodic arrays of Si cylinders (diameter 100-120 nm; height 240 nm) on the bottom, were placed on a front- and back-contacted Si heterojunction solar cell using immersion index matching fluid. The integrated design is shown in Fig. 3. The nanoscatterer array was fabricated by substrate conformal imprint lithography (SCIL).

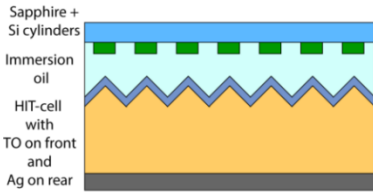


Figure 3: Schematic of silicon nanoscatterer arrays on bottom of a sapphire cover slide, integrated into a silicon heterojunction solar mini-module using immersion oil. The sapphire slide and the immersion oil mimic commonly used module glass and EVA.

Figure 4 (taken from [1]) shows the measured scattering spectrum of the integrated Mie scattering design. A clear resonance (peak amplitude 35-40%), due to the magnetic (550 nm) and electric (528 nm) dipole resonances is observed [9,10]. Reference measurements for a bare Si heterojunction solar cell and the unpatterned module are also shown. The bare cell shows low reflection due to the combination of texture and optimized AR coating (interference minimum at ~ 630 nm). The unpatterned module has a reflectivity of 7-12 % as expected given the refractive index for sapphire. The inset in Fig. 4 shows a photograph of the 12x12 mm² sapphire slide with the green reflecting Mie scattering design on top of the HIT solar cell. The green scattering intensity is quite insensitive to variation in incoming angle. For more details, see [1].

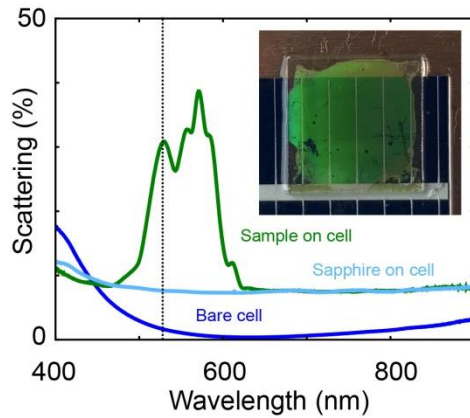


Figure 4: Measured scattering efficiency (green) of integrated design. Data for an unpatterned mini-module (light blue) and the bare Si heterojunction solar cell (dark blue) are also shown. Vertical black dashed line at $\lambda=528$ nm marks the electrical dipole resonance. Inset: Photograph of nanopatterned module shows bright green reflectance. Sapphire sample is 12x12 mm. Image taken from [1].

4 MIXED COLOR PIXELS

As described in Section 2, by variation of the size and density of the nanocylinders, the reflected color can be tuned to the desired spectral color range. To achieve mixed colors or white, we combine pixels of different colors, with each pixel composed of 50x50 μm^2 nanocylinder arrays. Figure 5 shows SEM images of the blue (radius 50 nm) and red (radius 90 nm) scattering random nanocylinder arrays. A random geometry was implemented to avoid diffraction effects for large scattering angles.

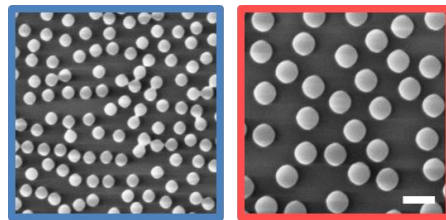


Figure 5: SEM top image of random Si nanocylinder arrays on sapphire, scattering in blue (left) and red (right). Scale bar is 500 nm.

In Figure 6, the measured scattering spectra of the blue and the red fields are shown (blue and red solid lines). The blue spectrum shows a weak resonance around 500 nm, the red spectrum shows strong first order resonances (electric and magnetic) around 800 nm and higher order resonances at 480 and 580 nm. The chromaticity values in the CIE 1931 xyY color space of the blue and red fields were determined by the concept described in Section 2 (see caption of Fig. 6).

In order to obtain a chromaticity close to white by combining red (r) and blue (b) pixels, the ratio of the red and blue pixel coverage r:b was chosen so that the xy values match the white point of the CIE 1931 color space of D65 ($x_{\text{White}}=0.3127$, $y_{\text{White}}=0.3290$). The chromaticity values x_n and y_n of the combined color can be determined by:

$$(x_n, y_n) = (x_b, y_b) \frac{bB_b}{B_n} + (x_r, y_r) \frac{rB_r}{B_n}$$

with the brightness of the blue array $B_b = X_b + Y_b + Z_b$, the red array $B_r = X_r + Y_r + Z_r$ and the combined brightness of the mixed fields $B_n = B_b + B_r$ [11]. Using the xyY values determined for the reflection spectra, we find that a pixel coverage ratio of r:b=1:3 leads to chromaticity values of $x_n=0.3181$ and $y_n=0.3283$, close to the white point.

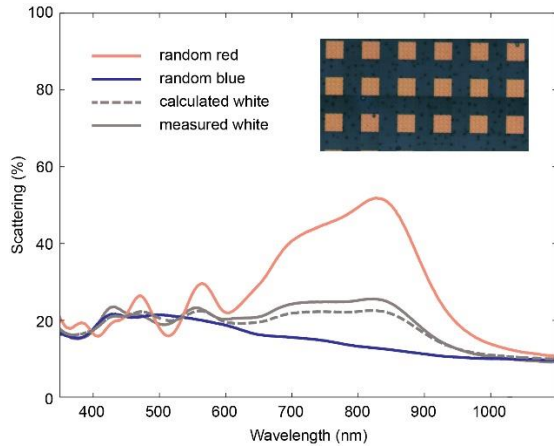


Figure 6: Measured scattering efficiency of blue and red reflecting random nanoarrays (blue and red solid lines). Spectra for calculated combined field (dashed grey line) and measured combined field (solid grey line) with ratio r:b=1:3. The chromaticity values of the plotted scattering curves are ($x_r=0.3868$, $y_r=0.3573$, $Y_r=0.3160$) for the red spectrum, ($x_b=0.2813$, $y_b=0.3128$, $Y_b=0.1718$) for the blue spectrum, ($x_{cw}=0.3181$, $y_{cw}=0.3283$, $Y_{cw}=0.2078$) for the calculated combined spectrum and ($x_{mw}=0.3281$, $y_{mw}=0.3323$, $Y_{mw}=0.2221$) for the combined measured spectrum. Inset: Optical microscope image of combined field. One red pixel and three blue pixels build a unit cell. Pixel is $50 \times 50 \mu\text{m}^2$.

Combining the two reflectance spectra in the ratio 1:3, and applying the method to determine the CIE color space values gives the dashed calculated line in Fig. 6. Next, the fields are combined experimentally in pixels of $50 \times 50 \mu\text{m}^2$ (see microscope image in inset of Fig. 6). The measured scattering spectrum (solid grey line in Fig. 6) of this combined field matches well the calculated scattering curve; resonance peaks are matching well over the entire spectral range. The reflected scattering spectrum of the mixed pattern has an average intensity of 22 % over the visible spectral range (450-800 nm)

5 TOWARDS A WHITE SOLAR CELL

Using the same approach as described in Section 4, a white colored solar mini-module was created. In these experiments the height of the nanocylinders was slightly smaller. Red to blue pixels had the optimized ratio r:b=1:9, and are shown in the microscope image in the inset of Fig. 7. The scattering spectra of the white integrated design, shown in Fig. 7, shows an average intensity of 20 % over the visible spectral range. The chromaticity values obtained from the scattering measurement of the nanopatterned module with combined red and blue fields are ($x=0.3320$, $y=0.3491$, $Y=0.2152$) and are close to the white point.

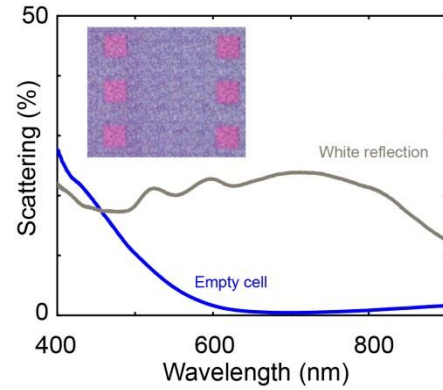


Figure 7: Measured scattering efficiency (grey) of integrated design of white field composed red and blue pixels. A spectrum for the bare Si heterojunction solar cell (dark blue) is also shown. Inset: Optical microscope image of combined field. One red pixel and 9 blue pixels are building a unit cell. Pixel is $50 \times 50 \mu\text{m}^2$.

Figure 8 shows the measured external quantum efficiency (EQE) of the nanopatterned mini-module and the bare Si solar cell. The EQE spectrum for the integrated design shows a reduction (15%-40%) over the entire visible spectrum up to 800 nm, resulting from light scattering and absorption by the Si nanoscatterers. The reduction observed above 800 nm is due to the reflection off the sapphire substrate. Correspondingly, the calculated J_{sc} is reduced by 25% (relative) from 40.8 to 30.7 mA/cm^2 compared to the bare Si heterojunction cell. Compared to the unpatterned module this would mean a relative reduction by 19%, taking into account 7% reflection from the sapphire slide.

One way to decrease the losses in this configuration is to tune the resonance of the red field, in order to have less reflection above 700 nm, as any reflection in that spectral range cannot contribute to the color perception, but reduces the short circuit current. A photograph of the white sample is depicted in the inset of Fig. 8. The color appearance is grey, which matches the measured spectra, as grey has the same chromaticity as white but is less luminescent. The brightness of the structure could be increased by increasing the scattering intensity of the pixels respectively.

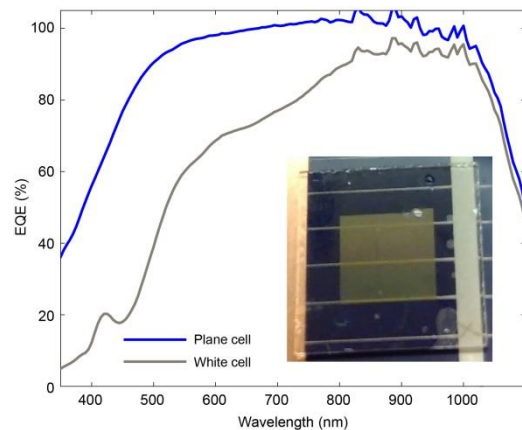


Figure 8: Measured EQE of bare silicon heterojunction solar cell (dark blue) and nanopatterned module with combined red and blue fields (grey). Inset: Photograph of nanopatterned module shows grey reflection. Sapphire sample is $12 \times 12 \text{ mm}$.

6 CONCLUSION

In this paper, we expanded the technology to create efficient bright green colored solar mini-modules to additional colors and white. We demonstrated the colored fabricated solar mini-module with a white scattering surface using pixels of integrated random nanoarrays. The concept can be widened to any desired color. The colored solar modules presented here can find applications in building- and landscape-integrated photovoltaics of many different kinds.

7 METHODS

7.1 Fabrication - Electron beam lithography

Silicon-on-sapphire substrates (500 nm Si on 0.46 mm sapphire, MTI Corporation) were etched down to a thickness of 200 nm using reactive ion etching (RIE) in a HBr_2 (25 sccm) and O_2 (2 sccm) plasma. For this, a 50 nm thick layer of HSQ was spincoated on top of a silicon-on-sapphire wafer and patterned with a dose of $3400 \mu\text{C}/\text{cm}^2$ in a Raith Voyager e-beam system. The samples were developed in TMAH (25%) for 60 seconds. Two subsequent RIE etch steps were performed, first to break through the sol-gel pattern using CHF_3 (25 sccm) and Ar (25 sccm), and second, to transfer the pattern into the silicon layer using HBr_2/O_2 .

7.2 Fabrication – SCIL

The Silicon-on-sapphire substrates were etched down in the way described in section 7.1. Next, we used substrate conformal imprint lithography (SCIL) to fabricate arrays of silicon cylinders. A 45-nm-thick silica sol-gel film was spin-coated and patterned using a SCIL stamp that was made from a pre-patterned silicon master, fabricated by electron-beam lithography. To transfer the pattern in the Si, the same etching steps as described in section 7.1 were performed

7.3 Reflectance measurements

Measurements were performed with an integrating sphere in reflection configuration. A collimated beam from a supercontinuum light source was coupled in at an incidence angle of 8° . In this setup, all light that is scattered/reflected from the sample in the upper hemisphere is collected and sent to a spectrometer.

7.3 EQE measurements

The active-area EQE spectrum was measured using slightly focused light (2 mm diameter) under normal incidence from a Xenon light source sent through a monochromator. The EQE of the bare Si heterojunction cell approaches 100% in the 600-900 nm spectral range.

8 ACKNOWLEDGMENTS

We gratefully acknowledge Paula Bronsveld and her team for fabricating the Si heterojunction solar cells, Marc Verschuuren for help with substrate conformal imprint lithography (SCIL), the assistance of Dmitry Lamers and Bob Drent for cleanroom support and Mark Knight for useful discussions. This work is part of the research program of the Netherlands Foundation for Scientific Research (NWO); it is also funded by the

European Research Council.

9 REFERENCES

- [1] V. Neder, S. L. Luxembourg, and A. Polman, *Applied Physics Letters*, 111, 073902 (2017).
- [2] J. Van De Groep and A. Polman, *Opt. Express* 21,26285 (2013).
- [3] E.-H. Cho, H.-S. Kim, B.-H. Cheong, P. Oleg, W. Xianyua, J.-S. Sohn, D.-J. Ma, H.-Y. Choi, N.-C. Park, and Y.-P. Park, *Opt. Express* 17, 8621 (2009).
- [4] L. Cao, P. Fan, E.S. Barnard, A.M. Brown, and M.L. Brongersma, *Nano Lett.* 10, 2649 (2010).
- [5] S. Sun, Z. Zhou, C. Zhang, Y. Gao, Z. Duan, S. Xiao, and Q. Song, *ACS Nano* 11, 4445 (2017).
- [6] J. Proust, F. Bedu, B. Gallas, I. Ozerov, and N. Bonod, *ACS Nano* 10, 7761 (2016).
- [7] Y. Kanamori, T. Ozaki, and K. Hane, *Opt. Express* 22, 25663 (2014).
- [8] J. Henrie, S. Kellis, S.M. Schultz, and A. Hawkins, *Opt. Express* 12, 1464 (2004).
- [9] A.I. Kuznetsov, A.E. Miroshnichenko, Y.H. Fu, J. Zhang, and B. Luk'yanchuk, *Sci. Rep.* 2, 1 (2012).
- [10] A.I. Kuznetsov, A.E. Miroshnichenko, M.L. Brongersma, Y.S. Kivshar, and B. Luk'yanchuk, *Science* (80). 354, (2016).
- [11] SemanticScholar, "Perceiving Color 5.1 the Color Stimuli" (2008).